JOURNAL OF MATERIALS SCIENCE 28 (1993) 4767–4774

Influence of weld parameters on the mechanical properties of spot-welded Fe–Mn–Al–Cr alloy

C. J. LIN, J. G. DUH
Department of Materials Science and Engineering, National Tsing Hua University, Hsinchu, Taiwan 300

M. T. LIAO
National Yuen Lin Polytechnic Institute, Yuen Lin, Taiwan

The static weld strength, hardness and microstructure evolution of a Fe–Mn–Al–Cr alloy during spot welding were investigated. A nugget can be formed for weld times as low as 5 cycles at 60 Hz (83 ms). The nugget growth rate is different between the front and the rear of the acceptable weld region. In the acceptable weld region, the tensile-shear strength ranges from 3038 to 3626 N, and the cross-tension strength varies from 2356 to 3136 N. The static weld strength strongly depends on the nugget size, and the dependence of the static weld strength on the electrode force is affected by the weld time and weld current. Evolution of spot-welded nuggets indicates that the hardness in the nuggets is, on average, about 100 H_V higher than that in the base unwelded metal, which is attributed to a cooling effect after welding.

1. Introduction

Fe–Mn–Al based alloy systems have attracted a lot of research attention due to their potential as a substitute for conventional Fe–Ni–Cr stainless steels. The combination of manganese and carbon acts as an austenitic stabilizer which extends and stabilizes the gamma loop in iron and retains the face-centered-cubic austenitic phase [1–3]. Recent research on the development of Fe–Mn–Al systems has included the effect of carbon and chromium on the high-temperature-oxidation behaviour, the oxidation induced phase transformations and the nitriding kinetics [4–11]. The results show promise for Fe–Mn–Al-based alloys to be substituted for conventional Fe–Ni–Cr systems. However, the weldability of the alloy must be assessed, if this new alloy is to be used in practical applications. Chou and Lee [12–14] examined Fe–29% Mn–8% Al–x% C ($x = 0.5$, 0.8, 1.1) alloys welded by gas-tungsten arc welding (GTAW). Both U-bend and tensile specimens exhibited excellent strength (>900 MPa) and ductility (>20%). They also observed that the carbon content exerted a strong influence on the residual ferrite. Recently, a preliminary study of the weldability of Fe–Mn–Al-based alloys has been carried out [15], and the purpose of this paper is to investigate further the welding behaviour of Fe–Mn–Al alloys. The tensile strength and hardness in spot-welded Fe–Mn–Al are discussed with respect to the weld current, cycle and electrode force.

2. Experimental procedures

The test specimen was prepared from pure Al, Mn, Cr and Fe, raw materials in an induction furnace and cast into a 1500 kg mould. The ingot was solution treated at 1150 °C for 4 h, and then hot rolled 20–30 times at 1150 °C until it was 3.5 mm thick, before it was cold rolled into a 1 mm thick sheet. Bright annealing took place at 1175 °C for 30 min under a H_2 reduction atmosphere. Table I shows the chemical composition of the material studied. The cold sheet was cut into sizes 30 × 100 mm and 50 × 150 mm for a tensile-shear test and a cross-tension test, respectively. Before welding, the specimens were ground with #400 SiC paper to a final thickness of 0.9 mm and then spot welded at 220 V, 60 Hz, at a maximum current of 20 000 A, with a truncated CF-type electrode tip as shown in Fig. 1. The variable experimental parameters included electrode force, weld current, and time.

The spot location and specimen size are shown in Figs 2 and 3. In Fig. 2, a single-spot test piece was produced to the specification JIS Z3136 in [16], and, in Fig. 3, to the specification JIS Z3137 in [17]. Both tests were carried out in accordance with JIS Z2241 [18]; and the maximum loads were measured. For each test, at least three specimens were employed.

Welded specimens were cut to reveal the cross-section of the nugget centre and then polished for microhardness measurement. The position of measurement is shown in Fig. 4a. The applied load to produce appropriate indentation was 50 g. The distance between every measurement point was 0.25 mm, and the reported data for each position was taken from the average by measuring three points which were 0.1 mm apart in the normal direction as shown in Fig. 4b.

0022–2461

TABLE 1 Chemical composition of the alloy studied

Element	Mn	Al	Cr	Mo	Si	C	Fe
Wt%	26.3	6.8	5.5	0.9	0.4	1.0	Balance

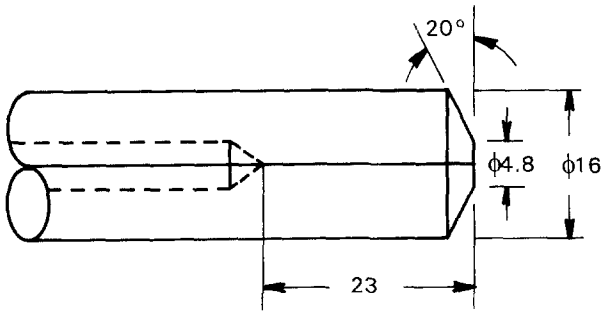

Figure 1 The shape of the electrode tip.

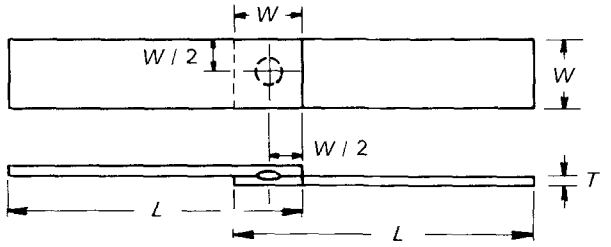

Figure 2 The shape and dimensions of the tensile-shear test piece. $W = 30$ mm, $L = 100$ mm, and $T = 1.0$ mm.

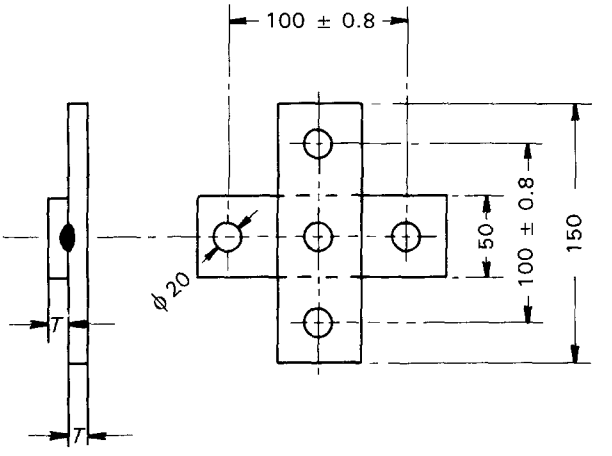

Figure 3 The shape and dimensions of the cross-tension test piece. The lengths are in millimetres.

3. Results and discussion

Weld-nugget morphologies are shown in Figs 5–7, as a function of electrode force, weld time and current, respectively. In Fig. 5, the nugget size at a 1470 N electrode force (welded under 15 cycles weld time at 60 Hz (250 ms), for a 3.8 kA average weld current and 30 cycles (500 ms) hold time is somewhat smaller than those welded at 2058 N and 2842 N. Fig. 6 illustrates the nugget development as a function of the weld time under a 2058 N electrode force, a 3.95 kA average weld current and 30 cycles (500 ms) hold time. It appears that the nugget becomes larger as the weld

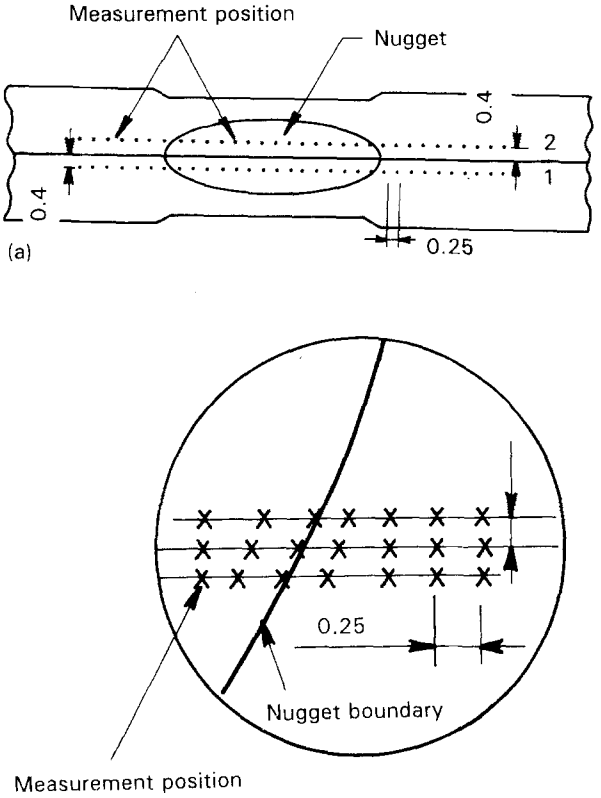

Figure 4 Schematic diagram for the measurement position for micro-hardness. The distances are in millimetres.

time is increased. It is observed that the nugget forms even when the weld time is as low as 5 cycles (83 ms), although it is relatively small in size. However, no significant change in nugget size is observed from 10 (166 ms) to 20 cycles (333 ms) weld time at 60 Hz. It should be pointed out that a region of very rapid nugget growth prevails from 5 (83 ms) to 10 weld cycles (166 ms) despite this, no nugget is formed below 5 cycles (83 ms) weld time. Between 10 weld cycles (166 ms) and expulsion, the rate of nugget growth dramatically decreases. Similar phenomena were found by Gould in a study of nugget development during resistance spot welding of AISI 1008 [19]. Fig. 7 indicates the nugget-size variation as a function of weld current under a 2058 N electrode force, for 15 cycles (250 ms) weld time and 30 cycles (500 ms) hold time. In this case, 3.48 kA is the minimum acceptable current and 6.75 kA is the maximum acceptable current [15], beyond which an expulsive failure mode is observed. The nugget size increases then approaches a steady state, as the weld current increases. Quantitatively speaking, the dependence of indentation on weld current is similar to that of nugget size on weld current. As a comparison, for a 300 series austenitic stainless steel 0.9 mm thick, the nugget was formed as low as 6 cycles at 60 Hz (100 ms) weld time for spot welding. However, the welding current increased from 5.5 kA to 7.3 kA at 3528 N electrode force [20]. The shear strength of a 300 series austenitic stainless steel was 3600 N, which is similar to the value in this study for Fe–Mn–Al–Cr alloy.

It should be pointed out that pores are observed in Figs 5–7. They are mostly distributed near the end of

the nugget. Due to the effect of electrode-tip pressure and previous solidification on the ends of nugget, gas cannot be released from the melting pool immediately and thus pores are formed.

The tensile-shear test is one of the most important methods in examining a single-spot weld. The generally accepted industry standards of resistance spot welds for plain carbon steels require a maximum fusion diameter and a minimum shear strength for a given metal gauge [21]; and with destructive testing only the parent metal around the weld may fail. Vanden Bossche [22] proposed the requirements of size, strength and failure modes which have become the basic weldability criteria for sheet steels used in automotive components. Fig. 8 shows the normal (pull-out) failure and interface failure after a tensile-shear test. In these two markedly different failure modes of spot welds, the interface fracture is considered unacceptable for a spot weld.

The tensile-shear strength (TSS) of spot welds is plotted against nugget size at a 3.95 kA weld current and 10 cycles (166 ms) weld time under three different electrode forces in Figs 9 and 10. By increasing the nugget size, the static TSS increases. Herein, a knife-edged caliper was used to measure the button size. The nugget size is the average diameter and equal to

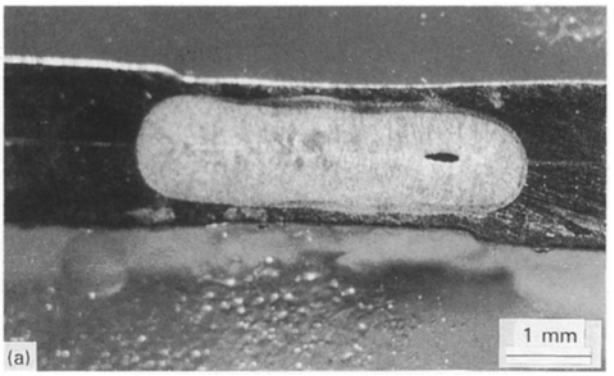

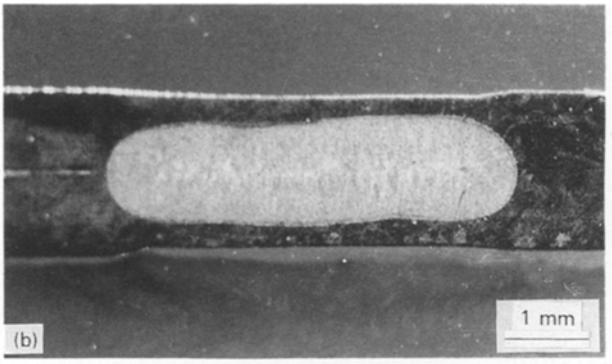

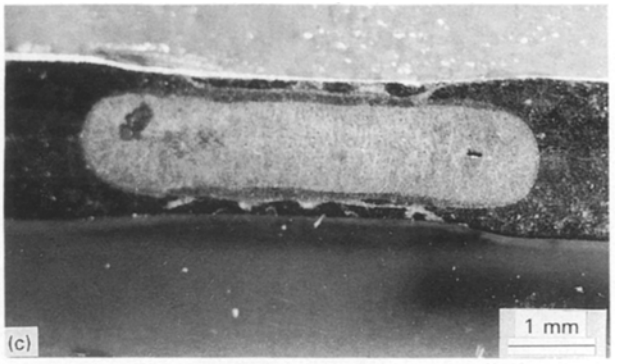

Figure 5 Micrographs showing nugget variation as a function of the following electrode forces for a weld time of 250 ms, a 3.8 kA weld current and a 500 ms hold time: (a) 1470 N, (b) 2058 N, and (c) 2842 N.

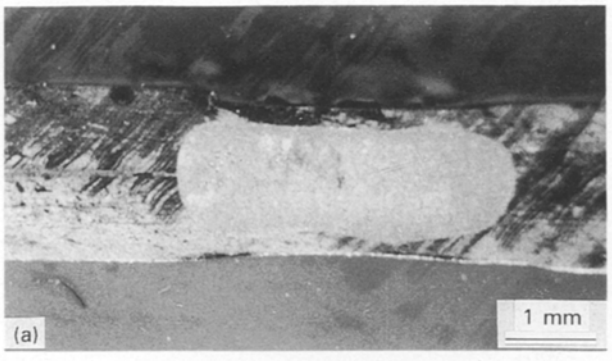

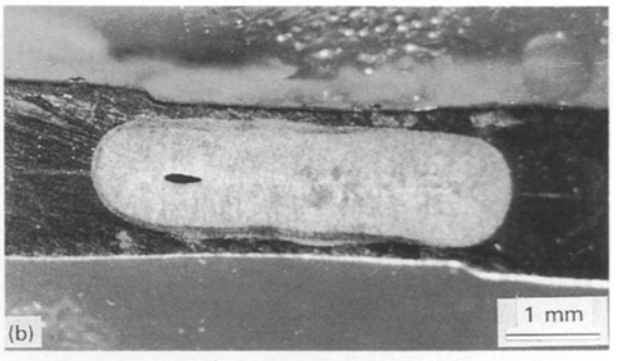

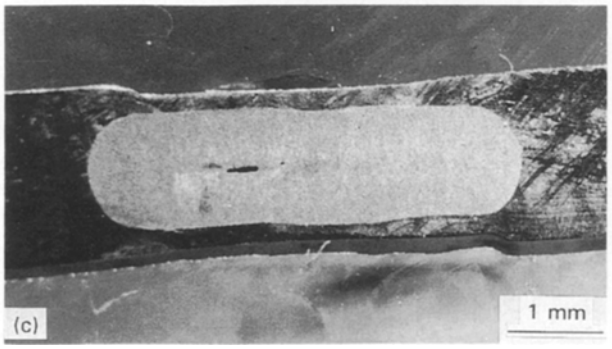

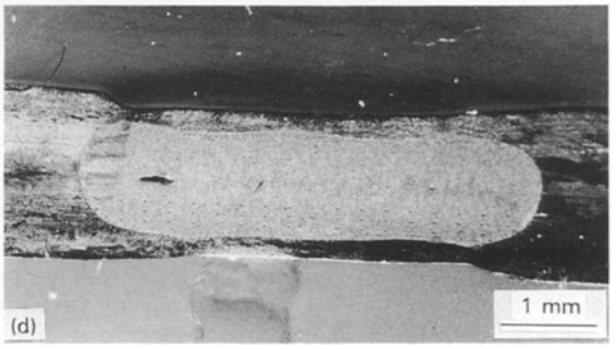

Figure 6 Micrographs showing nugget variation as a function of the following weld times at a 2058 N electrode force, a 3.95 kA weld current and a 500 ms hold time: (a) 83 ms, (b) 166 ms, (c) 250 ms, and (d) 333 ms.

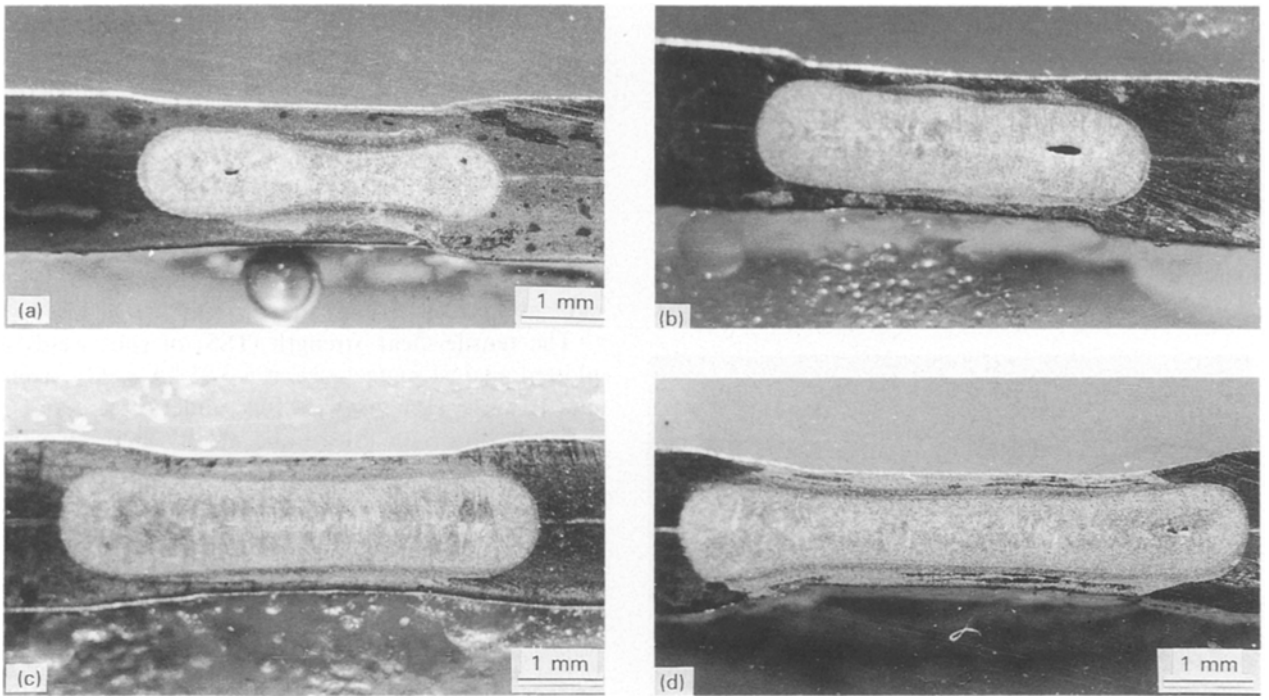

Figure 7 Micrographs showing nugget variation as a function of the following weld currents at a 2058 N electrode force, a 250 ms weld time and a 500 ms hold time: (a) 3.48 kA, (b) 3.78 kA, (c) 4.53 kA, and (d) 6.75 kA.

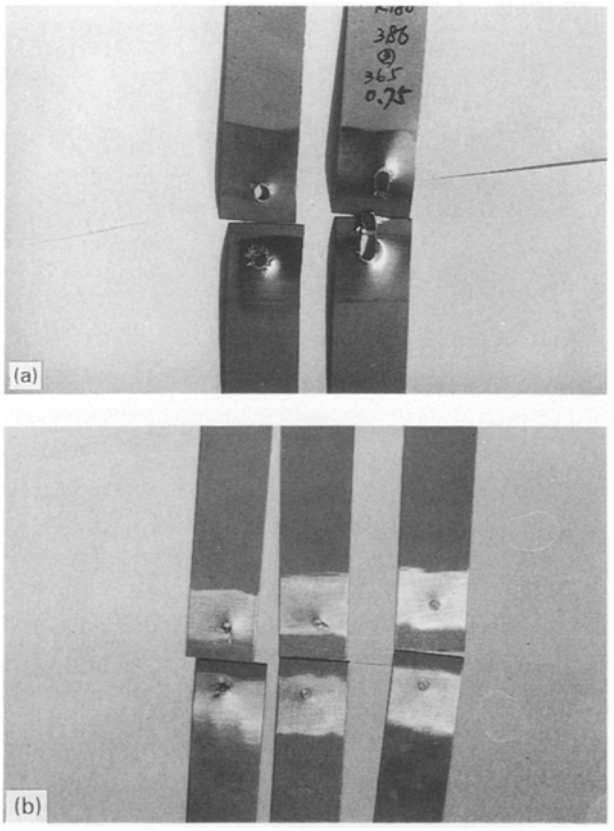

Figure 8 Micrographs showing tensile-shear failure: (a) normal failure, and (b) interface failure.

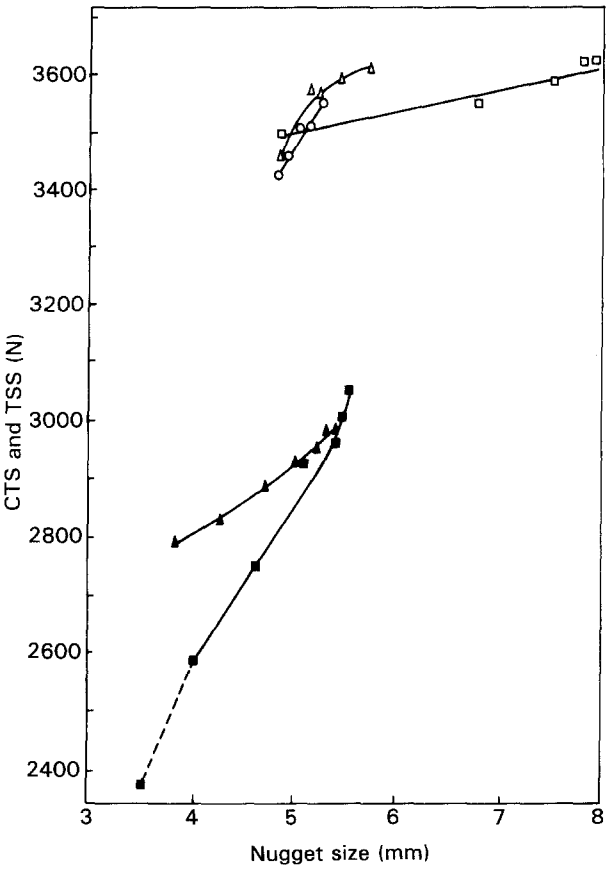

Figure 9 Tensile-shear strength (TSS) and cross-tension (CTS) strength as a function of nugget size at a 3.95 kA weld current: (—) normal failure, (- - -) interface failure, (□) 1470 N electrode force (TSS), (△) 2058 N electrode force (TSS), (○) 2842 N electrode force (TSS), (■) 1470 N electrode force (CTS), and (▲) 2058 N electrode force (CTS).

$(d + D)/2$, where d and D are the measured lengths of the nugget in perpendicular directions. Fig. 11 represents the relationship between the TSS and weld time under a 3.95 kA weld current for different electrode forces. It is interesting to note that a parabolic curve is observed for a 1470 N electrode force, while a more linear relation exists as the electrode force is increased to 2842 N. When the weld time is below 10 cycles (166 ms) the TSS is higher because the electrode force is larger. However, when the weld current goes beyond 10 cycles (166 ms), the larger the electrode force, the

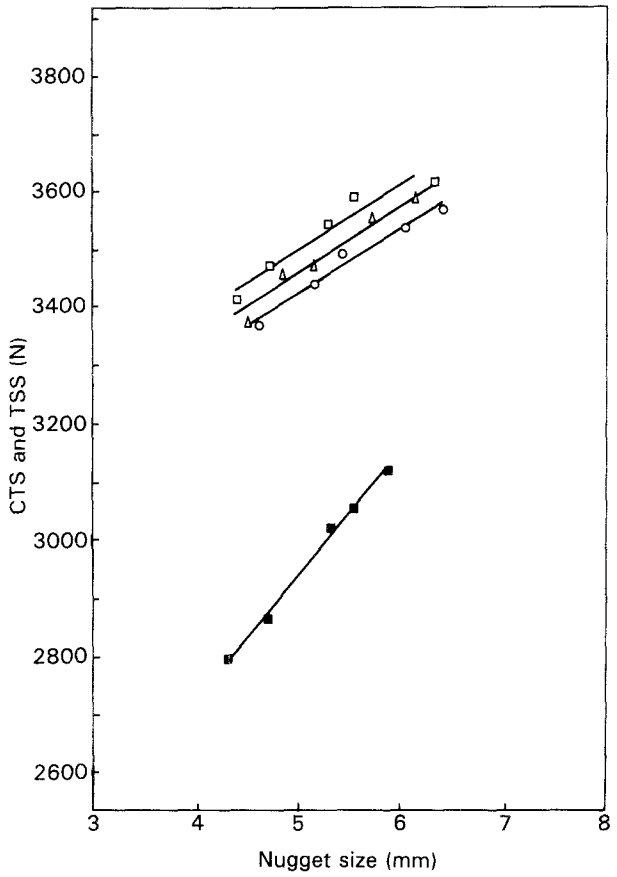

Figure 10 Tensile-shear strength and cross-tension strength as a function of nugget size at a 166 ms weld time: (□) 1470 N electrode force (TSS), (△) 2058 N electrode force (TSS), (○) 2842 N electrode force (TSS), and (■) 1470 N electrode force (CTS).

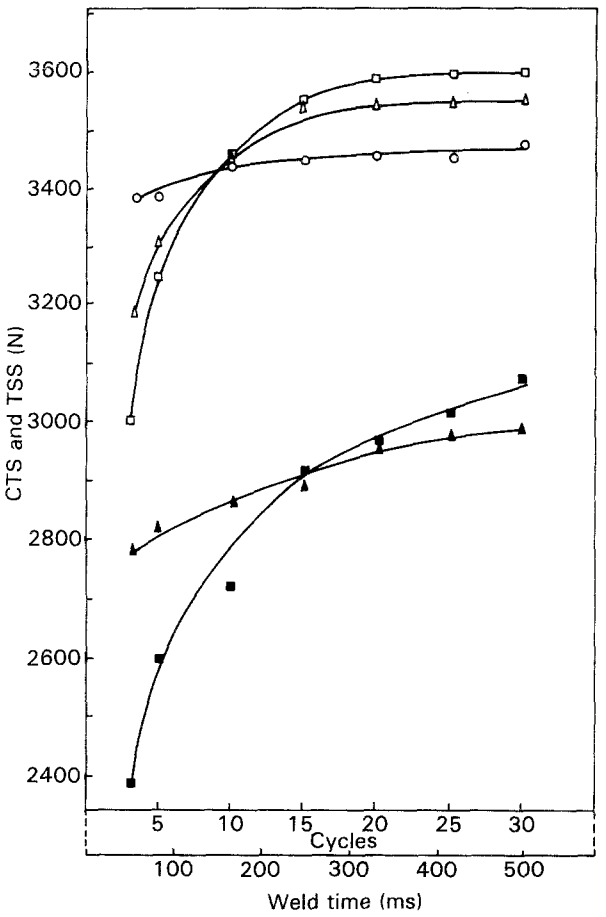

Figure 11 Tensile-shear strength and cross-tension strength as a function of weld time at a 3.95 kA weld current: (□) 1470 N electrode force (TSS), (△) 2058 N electrode force (TSS), (○) 2842 N electrode force (TSS), (■) 1470 N electrode force (CTS), and (▲) 2058 N electrode force (CTS).

lower the strength. By choosing 10 cycles (166 ms) as the reference weld time and replotting the TSS against the weld current, Fig. 12 is obtained, which clearly indicates that there is a simple relationship between TSS and weld current. It appears that the effect of electrode force is not significant. It should be pointed out that the dependence of measured strength on the welding time is similar to the trend of nugget growth shown in Fig. 6, in which the nugget grows rapidly for weld times below 10 cycles (166 ms) while the growth rates tend to slow down as the weld time is increased above 10 cycles (166 ms).

Several studies [22, 23] have demonstrated that the static TSSs of spot welds made in low-carbon mild steels, high-strength steels and micro-alloyed steels were dependent upon the following properties: the prior microstructure, thickness and yield strength of the sheet to be welded; the diameter of the nugget and electrode tip; and the strength of the weld metal and the restraint imposed by the material surrounding the weld. In general, the TSS would increase in proportion to the nugget size, weld time and weld current in an acceptable weld region. A similar dependence is observed in this study, although the influence of electrode force on the TSS is not appreciable, as indicated in Fig. 12.

Another method of investigating the static weld strength and ductility is the so called cross-tension test. Fig. 13 shows micrographs of button and normal failure after cross-tension testing. These are considered to be acceptable failure modes of spot welds. The cross-tension strength (CTS) is plotted against the nugget size under 3.95 kA weld current for different electrode forces in Fig. 9. The CTS is more dependent on the nugget size at a 1470 N electrode force than that at a 2058 N electrode force. At 10 cycles (166 ms) weld time and 1470 N electrode force, the CTS is linearly proportional to the nugget size as shown in Fig. 10. The relationship between the TSS and weld time and weld current is similar to the relationship of the CTS to the weld time and weld current; both are shown in Figs 11 and 12. A parabolic relationship between CTS and weld time is also observed. Below 15 weld time cycles (250 ms), the larger the electrode force the larger the CTS strength. However, the reverse trend is found above 15 cycles weld time. Pollard [24] reported that the relationship of CTS to the weld current for HSLA steels revealed two distinct regions: (i) a low-current region in which the CTS of the weld increased with weld current, and (ii) a plateau in which the CTS was essentially independent of the weld current. In the first region, the CTS was simply determined by the weld diameter, while in the second region the CTS was determined by the weld ductility. However, in this study, as indicated in Fig. 11, this transition phenomena is also observed for the CTS plotted against the weld time instead of the weld current.

Microhardness surveys of welds at different electrode forces, weld currents and weld times are shown in Figs 14–16. It appears that the nugget hardness is somewhat higher as the electrode force is increased. The interfacial region between the heat-affected zone and the nugget exhibits the highest hardness, while a softer zone prevails in the centre of the nugget. It is argued that the variation of hardness is due to the

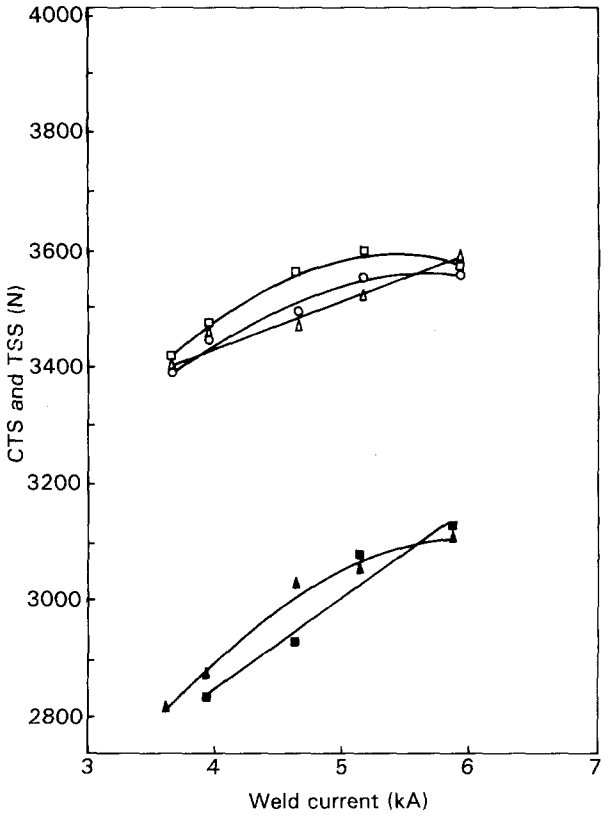

Figure 12 Tensile-shear strength and cross-tension strength as a function of weld current at 166 ms weld time: (□) 1470 N electrode force (TSS), (△) 2058 N electrode force (TSS), (○) 2842 N electrode force (TSS), (■) 1470 N electrode force (CTS), and (▲) 2058 N electrode force (CTS).

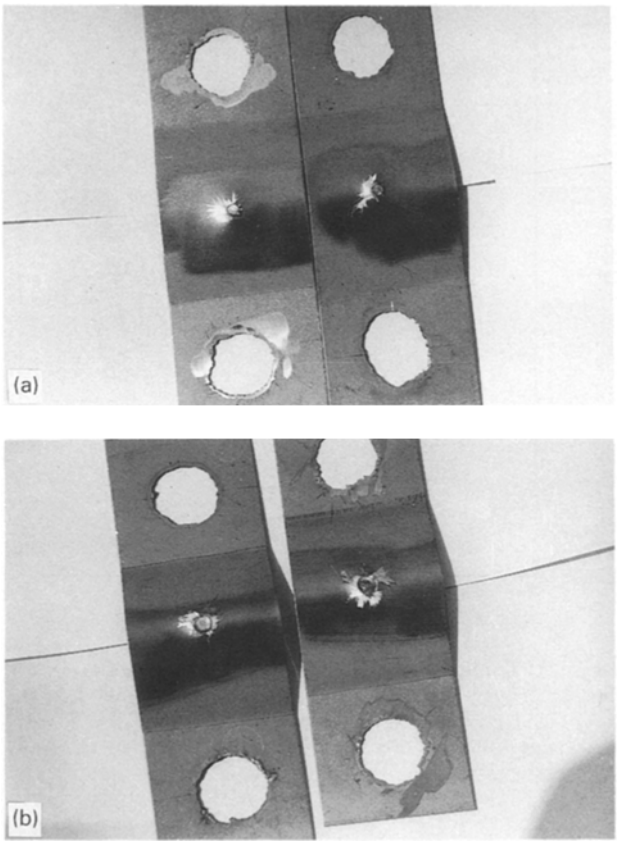

Figure 13 Micrographs showing cross-tension failure: (a) button failure, and (b) normal (pull-out) failure.

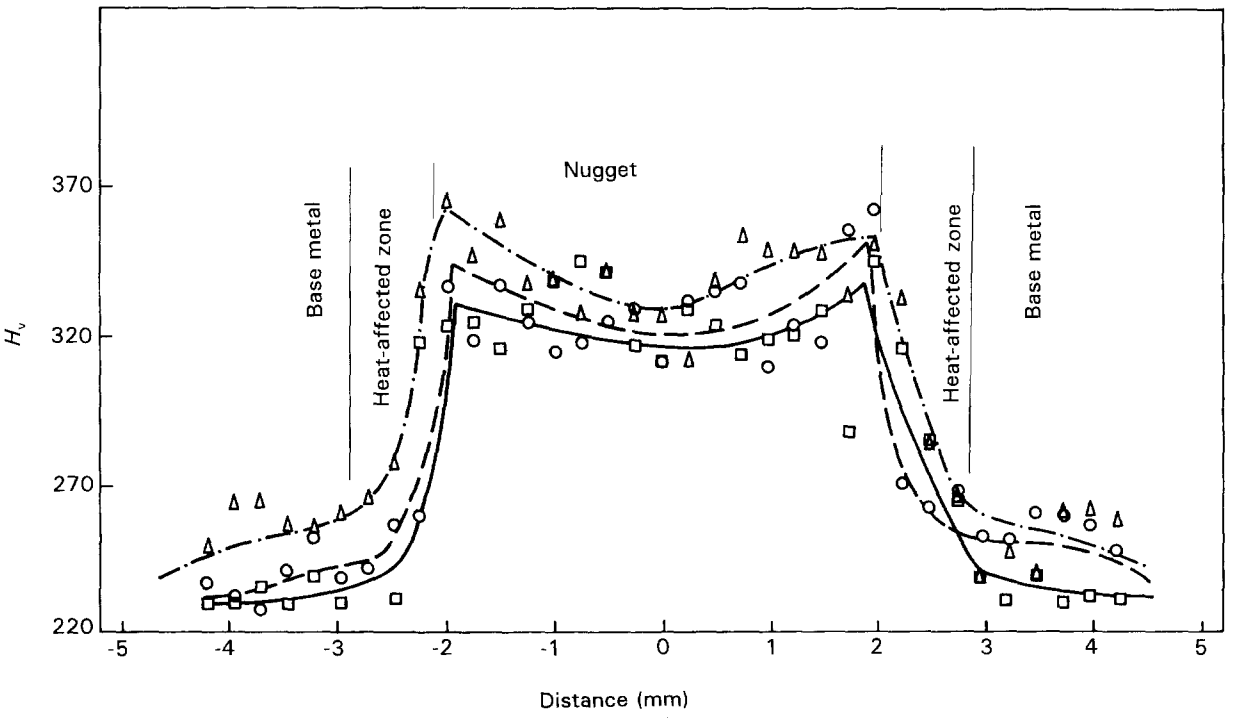

Figure 14 Hardness-value distribution traverse across the nugget at a 250 ms weld time and a 3.8 kA weld current for the following electrode forces: (□—□) 1470 N (○---○) 2058 N, and (△-·-△) 2842 N.

non-uniform cooling rate in different regions [25]. There is a greater distance for the metal in the centre of nugget from the water-cooled electrodes and the relatively large mass of heated metal in and around the weld, thus a slower quench rate is produced. As a consequence, the hardness is lower in the central region of the weld. In Fig. 15, for welds made at 2058 N electrode force and 15 cycles (250 ms) weld time, it is found that a 3.5 kA weld current introduces the highest hardness inside the nugget. It appears that the nugget hardness is slightly reduced as the weld current increases to 4.0, 4.5 and 6.75 kA, although the

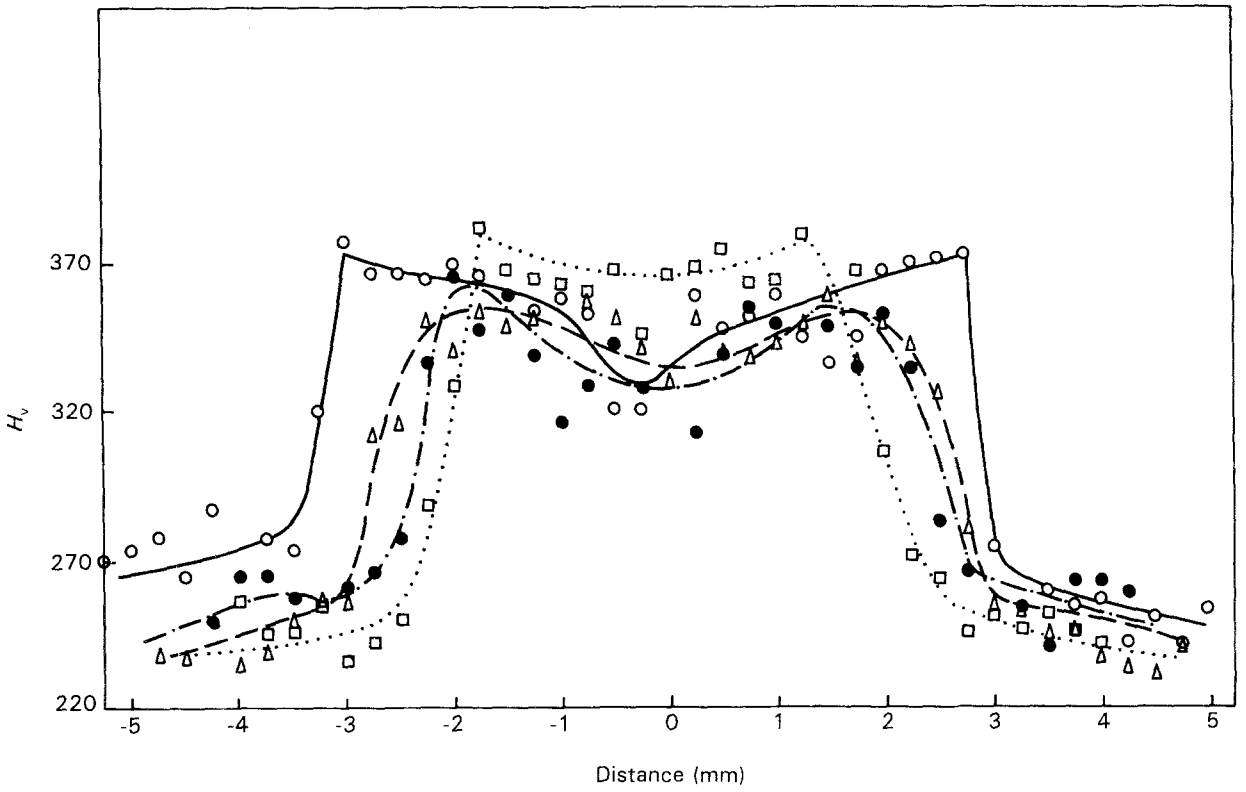

Figure 15 Hardness-value distribution traverse across the nugget at 2058 N electrode force and 250 ms weld time, for the following weld currents: (□···□) 3.5 kA, (●-·-●) 4.0 kA, (△---△) 4.5 kA, and (○—○) 6.75 kA.

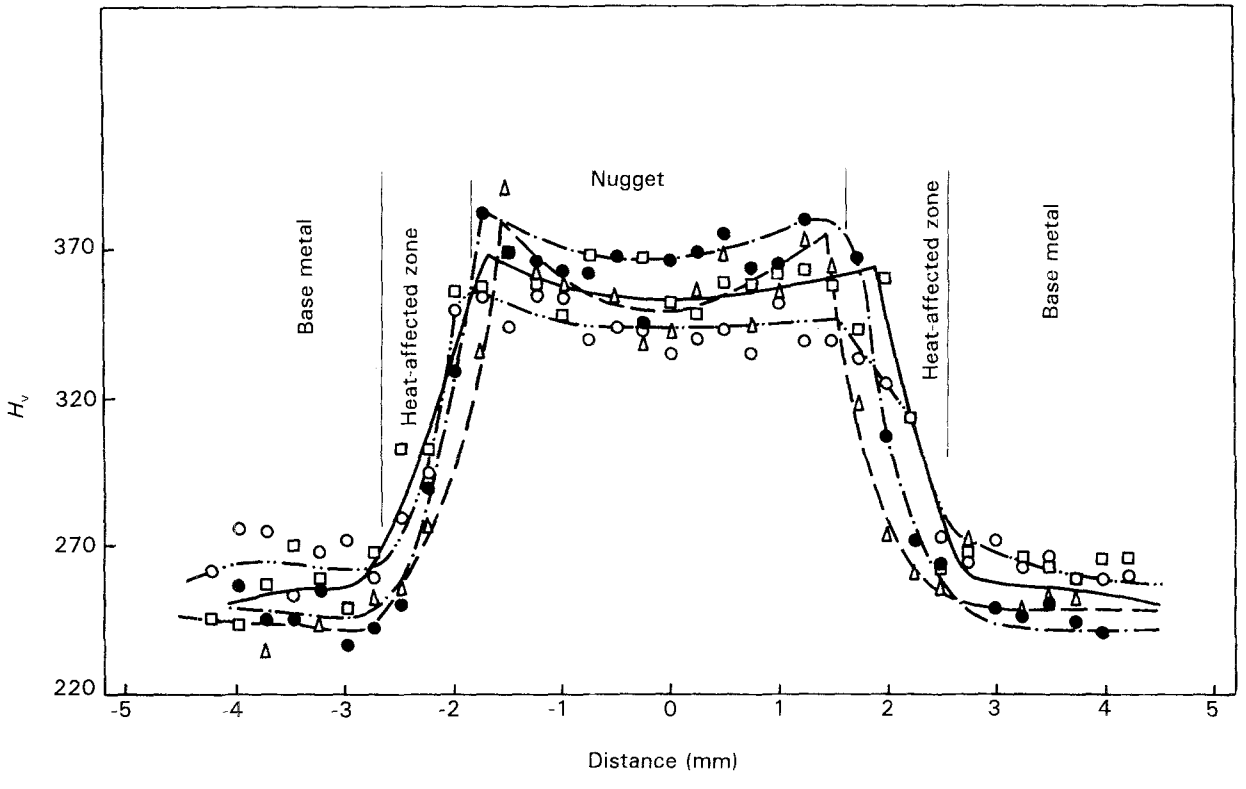

Figure 16 Hardness-value distribution traverse across the nugget at a 2058 N electrode force and a 3.8 kA weld current, for the following weld times: (△---△) 83 ms, (□—□) 166 ms, (●-·-●) 250 ms, and (○-··-○) 33 ms.

nugget size becomes larger as the weld current is increased.

For welds made at a constant 3.8 kA weld current and a 2058 N electrode force with various weld times, as shown in Fig. 16, the influence of the weld time on the heat-affected zone is not significant. It should be pointed out that as the weld time becomes >15 cycles (250 ms), an increase in the weld time not only degrades the TSS as illustrated in Fig. 11 but also decreases the nugget hardness as indicated in Fig. 16. If hardness value is the major concern, for welds made at a 2058 N electrode force and 3.8 kA weld current, 15 cycles (250 ms) weld time is the best condition. For welds made at a 2058 N electrode force and 15 cycles (250 ms) weld time the TSS and CTS are relatively lower than those made at currents higher than 3.5 kA, although a 3.5 kA, weld current presents the highest hardness in the nugget. However, if the weld current increases to 6.75 kA, not only is the nugget hardness practically constant at all values of weld current higher than 4.0 kA, as shown in Fig. 15, but the TSS and CTS are also enhanced as shown in Fig. 11. On the basis of the above observations, 15 cycles (250 ms) weld time seems to be the critical region in which the nugget hardness exhibits a value transition, although a steady-state strength is achieved as the weld time reaches 15 cycles (250 ms).

4. Conclusions

1. The mechanical properties of spot-welded Fe–Mn–Al–Cr alloys have been evaluated in this study. In the acceptable weld region, the TSS ranges between 2356 and 3136 N, with some porosity observed within the nugget.

2. A nugget is formed even when the weld time is as low as 5 cycles (83 ms) at 2058 N electrode force, 3.95 kA average weld current and 30 cycles (500 ms) hold time. The spot-weld strength strongly depends on the nugget size, and the strength is higher as the nugget size increases.

3. In the constant-weld-current condition, the TSS increases in proportion to the electrode force when the weld time is below 10 cycles (166 ms). Employment of a lower electrode force introduces a higher TSS when the weld time is above 10 cycles (166 ms). Similar relationships for the CTS dependence on the electrode force and weld time are also observed. The transition with weld time is, however, shifted to 15 cycles (250 ms).

4. In the constant-weld-time condition, both the TSS strength and CTS are enhanced as the weld current is increased. Nevertheless, the dependence of strengths on the electrode force is not significant.

5. The hardness of spot-welded nuggets is about 100 H_V higher than that of the base unwelded metal due to the cooling effect. In addition, the hardness is lower in the central region of nugget than in the edge of the nugget.

Acknowledgement

This study is partly supported by the National Science Council, Taiwan under contract No. NSC-81-0115-E-150-03.

References

1. S. K. BANERJI, "An Update on Fe–Mn–Al–Steels", Proceedings of the Workshop on "Conservation and substitution technology for critical materials", Vanderbilt University, Nashville, Tennessee, June 1981.
2. *Idem.*, "The 1982 Status Report on Fe–Mn–Al steels", presented at the public workshop on "Trends in critical materials requirements for steels of the future conservation and substitution technology for chromium", Vanderbilt University, Nashville, Tennessee, October 1982.
3. J. P. SAUER, R. A. RAPP and J. P. HIRTH, *Oxid. Met.* **18** (1982) 285.
4. C. J. WANG and J. G. DUH, *J. Mater. Sci.* **23** (1988) 769.
5. J. G. DUH, J. W. LEE and C. J. WANG, *ibid.* **23** (1988) 2649.
6. C. J. WANG and J. G. DUH, *ibid.* **23** (1988) 2913.
7. *Idem, ibid.* **23** (1988) 3447.
8. J. G. DUH and J. W. LEE, *J. Electrochem. Soc.* **136** (1988) 847.
9. J. G. DUH and C. J. WANG, *J. Mater. Sci.* **25** (1990) 268.
10. *Idem, ibid.* **25** (1990) 2063.
11. *Idem, ibid.* **25** (1990) 2615.
12. C. P. CHOU and C. H. LEE, *ibid.* **25** (1990) 1491.
13. *Idem, J. Mater. Sci. Engng A* **118** (1989) 137.
14. *Idem, Scripta Metall. A* **23** (1989) 901.
15. C. J. LIN, J. G. DUH and M. T. LIAO, submitted to *J. Mater. Sci.*
16. Japanese Standards Association, JIS Z3136, "Method of tension shear test for spot welded joint" (Japanese Standards Association, Tokyo, 1988).
17. Japanese Standards Association, JIS Z3137, "Method of tension test for spot welded joint" (Japanese Standards Association, Tokyo, 1988).
18. Japanese Standards Association, JIS Z2241, "Method of tensile test for metallic materials" (Japanese Standards Association Tokyo, 1984) 88.
19. J. E. GOULD, Welding Research Supplement, January (1987) 1s.
20. ASM, Metals handbook, 9th edn. Vol. 6 (American Society for Metals, Metals Park, Ohio, 1984) 525.
21. American Welding Society Document, "Recommended Practice for Resistance Welding", (1966) C1.1–66.
22. D. J. VANDEN BOSSCHE, Society of Automotive Engineers (1978) 955.
23. J-O Sperle, *Metal Construction* **15** (April 1983) 200.
24. B. POLLARD, Welding Research Supplement (August 1974) 343s.
25. W. F. HESS and D. C. HERRSCHAFT, Welding Research Supplement (October 1943) 451s.

Received 7 July 1992
and accepted 11 January 1993